Supplementary Information (SI) for Green Chemistry.

Chemical Looping Hydrogen Production from Ammonia and Water: Materials and Technoeconomics

Supplementary Information

Amirmohammad Arjomand Kermani[a], Kyle Shank[a], Shang Zhai*[a,b]

[a]Department of Mechanical and Aerospace Engineering, The Ohio State University, 201 West 19th Ave, Columbus, OH 43210, USA

[b]School of Earth Sciences, The Ohio State University, 125 South Oval Mall, Columbus, OH 43210, USA

*Corresponding author: Shang Zhai (zhai.218@osu.edu)

1. Experimental Methodology

1.1. Alumina-Supported Materials Synthesis

For alumina (Al_2O_3)-supported samples, $Fe(NO_3)_3.9H_2O$ (Sigma-Aldrich) and $Al(NO_3)_3.9H_2O$ (Sigma-Aldrich) were mixed with deionized water. The mass of the support material (Al_2O_3) was calculated to be 30% of the total mass of the fully oxidized sample. The solution was stirred on a hotplate at 300 rpm for ten minutes at ambient temperature; followed by the addition of concentrated sodium carbonate (Na_2CO_3) solution in deionized water (100 mL, 0.25 mol/L) to the nitrates solution while stirring. After 30 minutes of stirring at 300 rpm, the precipitate was separated by filtration and washed with deionized water. The obtained solid was dried in a furnace with air flowing (500 sccm) at 120°C overnight and calcined at 400°C for four hours[1]. The final product was further ground with a mortar and pestle. This sample is denoted as FeO_x/Al_2O_3. For the mixed iron-cobalt oxide, correct amounts of $Fe(NO_3)_3.9H_2O$ (Sigma-Aldrich) and $Co(NO_3)_2.6H_2O$ (Sigma-Aldrich), were mixed with the support following the same procedure. An example of the mixed cation oxide is noted as $Fe_{0.5}Co_{0.5}O_x/Al_2O_3$.

1.2. Materials Looping Performance Testing

The space velocity values were calculated using *Eq. S1* and *S2*, in which modifying the concentration of NH_3 gas to 1, 3, and 5% corresponded to 6, 18, and 30 $L_{NH_3}/(g_{solid}\,.h)$ respectively.

$$SV_{NH_3}[L_{NH_3}/(g_{solid}\,.h)] = \frac{\dot{V}_{NH_3}[{}^{standard\ mL}/_{min}] \times 60[{}^{min}/_{h}] \times 10^{-3}[{}^{L}/_{mL}]}{m_{solid}[g]} \qquad \textit{Eq. S1}$$

$$SV_{H_2O}[L_{H_2O}/(g_{solid}\,.h)] = \frac{\dot{V}_{H_2O}[{}^{standard\ mL}/_{min}] \times 60[{}^{min}/_{h}] \times 10^{-3}[{}^{L}/_{mL}]}{m_{solid}[g]} \qquad \text{Eq. S2}$$

The time-averaged conversions of NH_3 and H_2O were calculated via *Eqs. S3* and *S4* over five cycles, in which the molar flow rates of NH_3 and H_2O in the exhaust are integrated and divided by the integration of the inlet gas molar flow rate.

$$X_{NH_3} = \left(1 - \frac{\int_{t_1}^{t_2} \dot{n}_{NH_3,out}dt}{\int_{t_1}^{t_2} \dot{n}_{NH_3,in}dt}\right) \times 100\% \qquad \text{Eq. S3}$$

$$X_{H_2O} = \left(1 - \frac{\int_{t_1}^{t_2} \dot{n}_{H_2O,out}dt}{\int_{t_1}^{t_2} \dot{n}_{H_2O,in}dt}\right) \times 100\% \qquad \text{Eq. S4}$$

2. Looping Performance Experimental Results

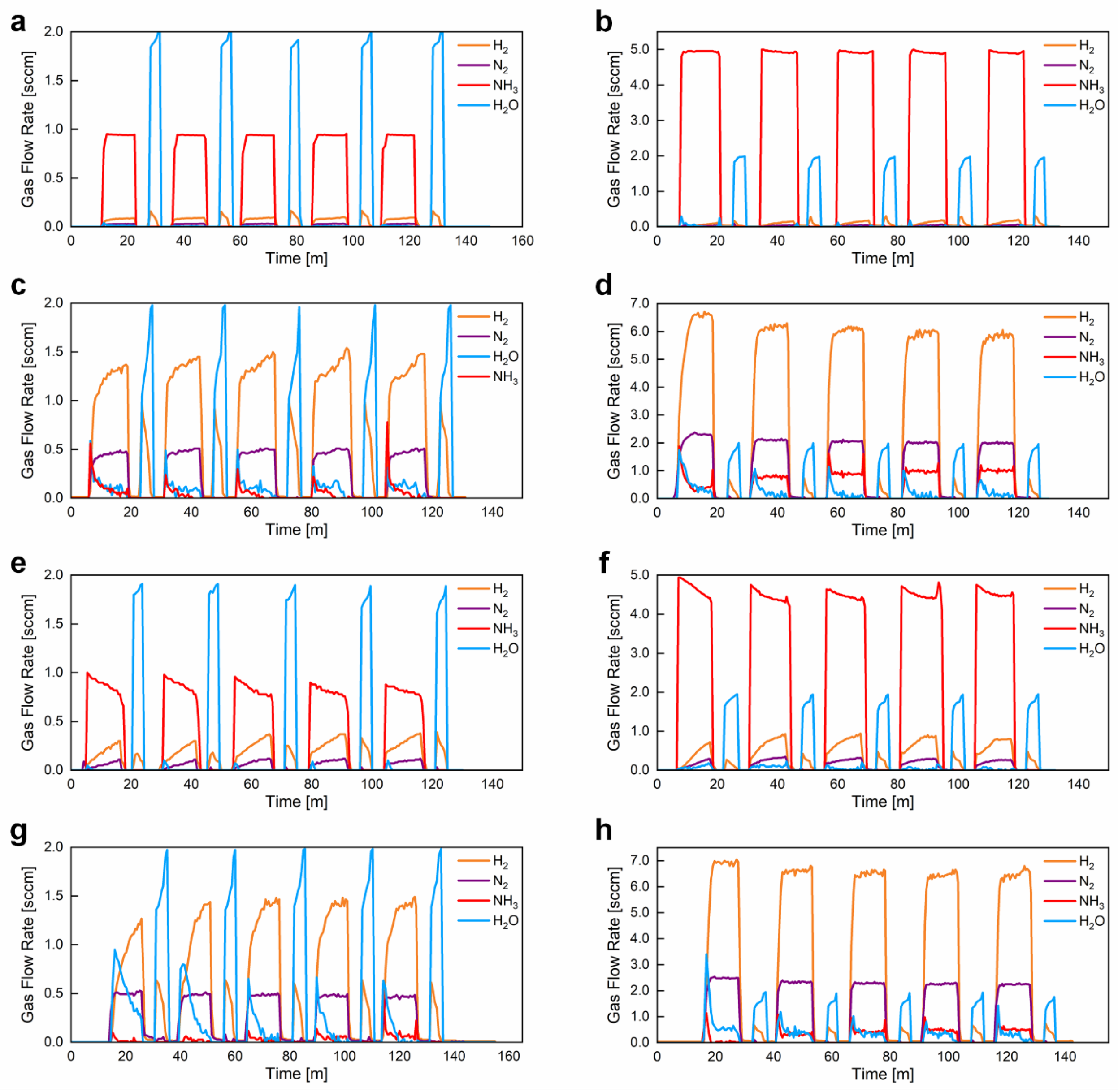

Figure S1: Reactor outlet gas profile of CLAOD-WS experiments using a) FeO$_x$/YSZ at 450°C and $\boldsymbol{SV_{NH_3}} = \boldsymbol{6\,L_{NH_3}/(g_{solid}\,.\,h)}$, *b) FeO$_x$/YSZ at 450°C and* $\boldsymbol{SV_{NH_3}} = \boldsymbol{30\,L_{NH_3}/(g_{solid}\,.\,h)}$, *c) FeO$_x$/YSZ at 600°C and* $\boldsymbol{SV_{NH_3}} = \boldsymbol{6\,L_{NH_3}/(g_{solid}\,.\,h)}$, *d) FeO$_x$/YSZ at 600°C and* $\boldsymbol{SV_{NH_3}} = \boldsymbol{30\,L_{NH_3}/(g_{solid}\,.\,h)}$, *e) Fe$_{0.5}Co_{0.5}O_x$/YSZ at 450°C and* $\boldsymbol{SV_{NH_3}} = \boldsymbol{6\,L_{NH_3}/(g_{solid}\,.\,h)}$, *f) Fe$_{0.5}Co_{0.5}O_x$/YSZ at 450°C and* $\boldsymbol{SV_{NH_3}} = \boldsymbol{30\,L_{NH_3}/(g_{solid}\,.\,h)}$, *g) Fe$_{0.5}Co_{0.5}O_x$/YSZ at 600°C and* $\boldsymbol{SV_{NH_3}} = \boldsymbol{6\,L_{NH_3}/(g_{solid}\,.\,h)}$, *h) Fe$_{0.5}Co_{0.5}O_x$/YSZ at 600°C and* $\boldsymbol{SV_{NH_3}} = \boldsymbol{30\,L_{NH_3}/(g_{solid}\,.\,h)}$. *For all of these experiments* $\boldsymbol{SV_{H_2O}} = \boldsymbol{12\,L_{H_2O}/(g_{solid}\,.\,h)}$.

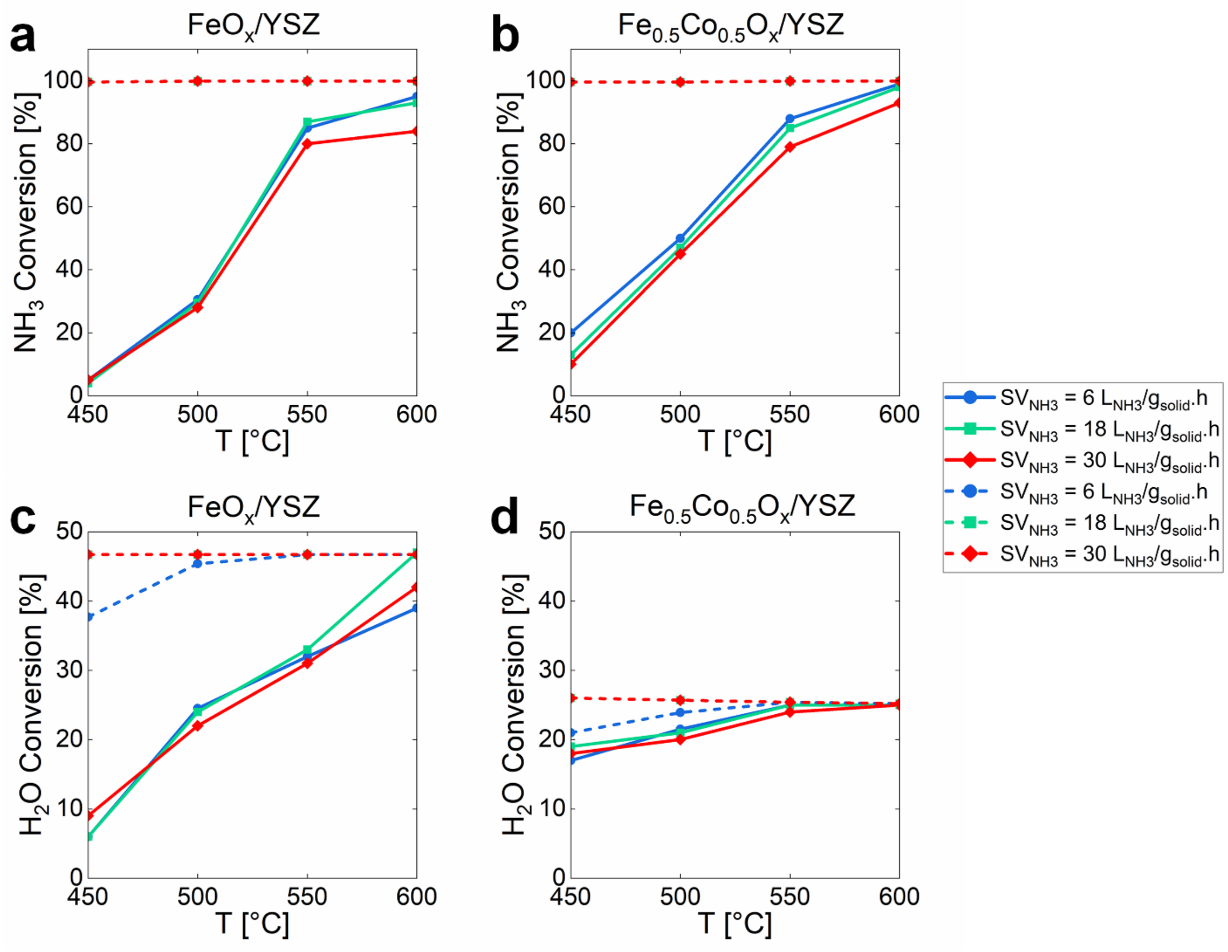

Figure S2: Looping performance of YSZ-supported materials at different NH$_3$ *step space velocities. Ammonia conversions of a) FeO*$_x$*/YSZ and b) Fe*$_{0.5}$*Co*$_{0.5}$*O*$_x$*/YSZ. Steam conversions of c) FeO*$_x$*/YSZ and d) Fe*$_{0.5}$*Co*$_{0.5}$*O*$_x$*/YSZ. Conversions are calculated using Eqs. S3 and S4. "max" refers to the thermodynamic equilibrium conversions and "exp" refers to five-cycle experimental results. For all results here,* $SV_{H_2O} = 12\, L_{H_2O}/(g_{solid}\, .h)$.

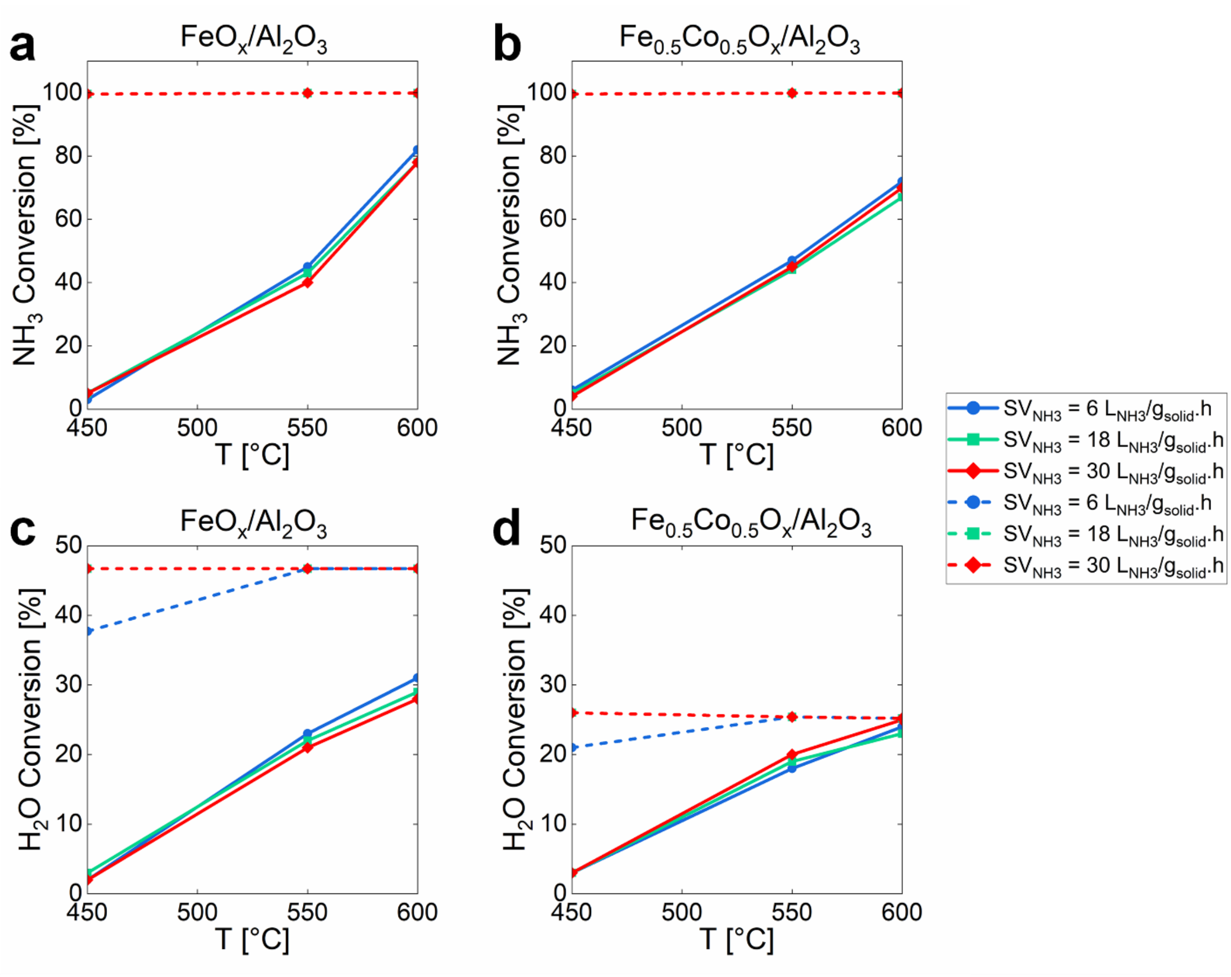

Figure S3: Looping performance of Al_2O_3 supported materials at different NH_3 step space velocities. Ammonia conversions of a) FeO_x/Al_2O_3 and b) $Fe_{0.5}Co_{0.5}O_x/Al_2O_3$. Steam conversions of c) FeO_x/Al_2O_3 and d) $Fe_{0.5}Co_{0.5}O_x/Al_2O_3$. Conversions are calculated using Eqs. S3 and S4. "max" refers to the thermodynamic equilibrium conversions and "exp" refers to five-cycle experimental results. For all results here, $SV_{H_2O} = 12\, L_{H_2O}/(g_{solid}\ .h)$.

Other materials were synthesized and tested for the CLAOD-WS at 600°C with 6 $L_{NH_3}/(g_{solid}\ .h)$ and 12 $L_{H_2O}/(g_{solid}\ .h)$ space velocities. The results are shown in *Table S1*. These samples were not further investigated due to their worse performance compared with FeO_x/YSZ and $Fe_{0.5}Co_{0.5}O_x$/YSZ.

Table S1: NH_3 and H_2O conversions of CoO_x/YSZ, NiO_x/YSZ, and $Fe_{0.5}Ni_{0.5}O_x$/YSZ in five cycles of CLAOD-WS at 600°C with 6 $L_{NH_3}/(g_{solid}\ .h)$ and 12 $L_{H_2O}/(g_{solid}\ .h)$ space velocities.

Material	NH_3 conversion [%]	H_2O conversion [%]
CoO_x/YSZ (30wt%)	95	2
NiO_x/YSZ (30wt%)	79	0
$Fe_{0.5}Ni_{0.5}O_x$/YSZ (30wt%)	62	12

It is worth mentioning that potentially small traces of NO_x gases (NO, NO_2, and N_2O) were detected in the NH_3 step of the first CLAOD-WS cycle for several samples, but no NO_x was detected beyond the first cycle *(Figure S4)*.

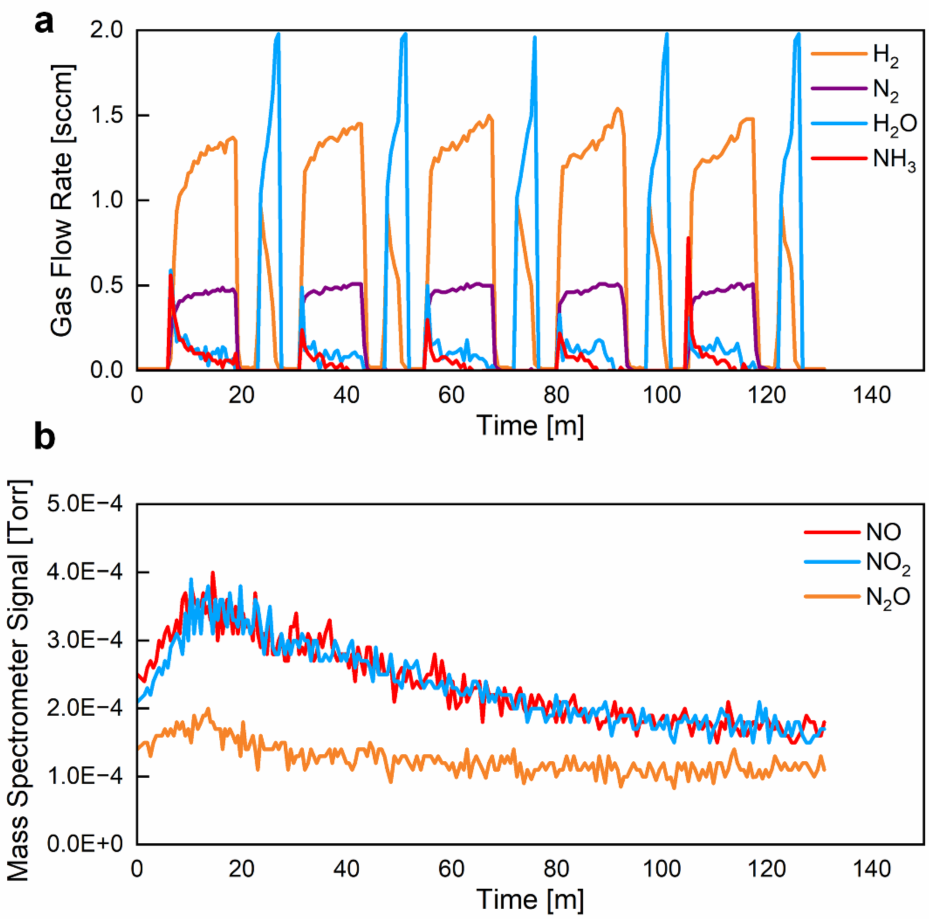

Figure S4: CLAOD-WS reactor outlet gas profiles using FeO_x/YSZ at 600°C: a) Quantified gas flow rates of H_2, N_2, H_2O, and NH_3 in sccm, and b) Mass spectrometer signals for NO, NO_2, and N_2O in Torr.

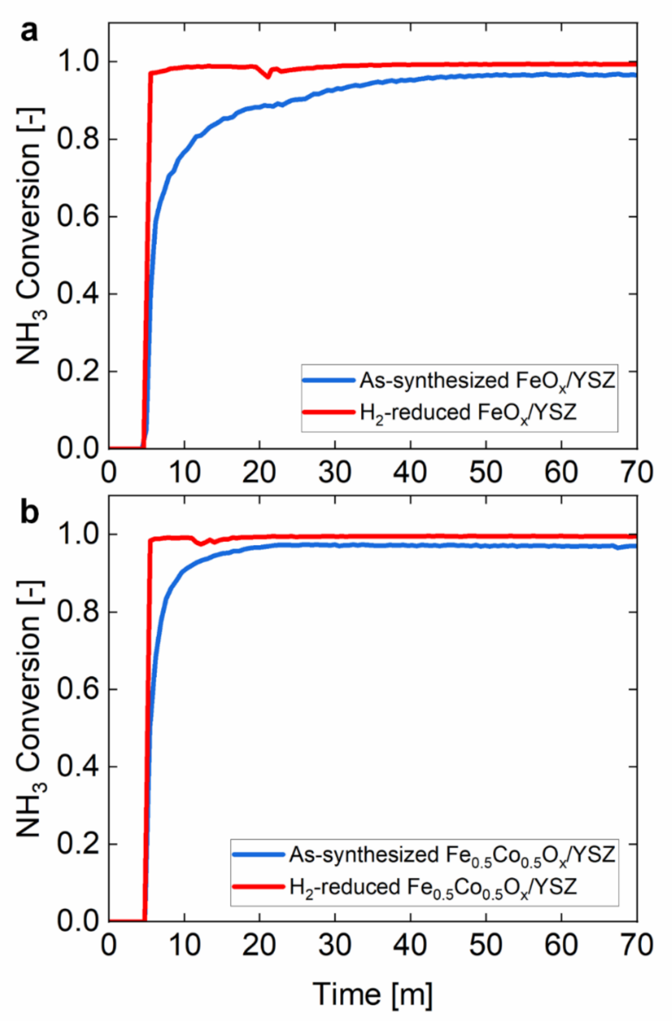

Figure S5: NH_3 conversion H_2-reduced (red) and as-synthesized (blue) a) FeO_x/YSZ and b) $Fe_{0.5}Co_{0.5}O_x$/YSZ at 600°C and $SV_{NH_3} = 6\,L_{NH_3}/(g_{solid}\,.h)$ *. The H_2 reduction was for 60 minutes, and the as-synthesized materials were fully oxidized by air at 600°C during synthesis.*

3. Equilibrium Simulations Using *Equilibrium* and *Phase Diagram* Modules in *FactSage*

To determine the phases at equilibrium, two steps of our presented looping scheme were separately simulated in the *Equilibrium* module of *FactSage* software[2, 3]. The reactants in the equilibrium calculation were defined as the same amount of solid as our experiment and the same amount of gases flown to the reactor over the duration of a reaction step (12 min for the NH_3 step, and 3 min for the steam step). For gases, the volume of gases flown to the reactor over the duration of a reaction step was divided by the molar volume of gases at standard conditions. Initially, specific molar amounts of reactant gases and solids for the NH_3 step were set up to reach equilibrium, giving equilibrium solid and gas compositions, and the resulting equilibrium pO_2. Then the resulting solid at equilibrium in the NH_3 step was taken to react with H_2O and reach equilibrium in the model, giving equilibrium composition and pO_2. These pO_2 values between reduced and re-oxidized states were shown as the range of phase transition on phase diagrams of Fe – O, and Fe – Co – O systems in *Figures 4i* and *4j*.

To plot phase diagrams, elements of Fe and O for the Fe – O system and Fe, Co, and O for Fe – Co – O system were input to the *Phase Diagram* module of *FactSage* software. For the Fe – O system, for a given range of temperature and p_{O2}, the phase diagram was plotted. For the Fe – Co – O system, for a given range of temperature and p_{O2}, the molar ratio of Fe/(Fe+Co) was set to be 0.5. For both material systems, the total system pressure was set to be 1 atm.

4. Material Characterization with XANES and Oxidation State Analysis

XANES data was analyzed by *Athena* software to give normalized absorption (μ) vs. absorption energy as in *Figures 5a to 5f*[4]. *Table S2* and *Figure S6a* show the oxidation states of Fe in FeO_x/YSZ in NH_3-reduced and steam-oxidized conditions at 450℃ and 600℃. Similarly, *Tables S3* and *S4* as well as *Figures S6b* and *S6c* show the oxidation states of Fe and Co in $Fe_{0.5}Co_{0.5}O_x$/YSZ in NH_3-reduced and steam-oxidized conditions at 450°C and 600°C, respectively. To evaluate the change in oxidation state per mol of active metal in $Fe_{0.5}Co_{0.5}O_x$/YSZ, oxidation state changes for Fe and Co were both included considering their molar ratio (*Table 1*).

Table S2: Oxidation state of Fe in FeO_x/YSZ according to XANES.

T [°C]	Oxidation state of Fe in FeO_x/YSZ		Oxidation state change
	Reduced	Re-oxidized	
450	1.38	2.69	1.31
600	0.00	2.86	2.86

Table S3: Oxidation state of Fe in $Fe_{0.5}Co_{0.5}O_x$/YSZ according to XANES.

T [°C]	Oxidation state of Fe in $Fe_{0.5}Co_{0.5}O_x$/YSZ		Oxidation state change
	Reduced	Re-oxidized	
450	1.31	3.00	1.69
600	0.00	3.00	3.00

Table S4: Oxidation state of Co in $Fe_{0.5}Co_{0.5}O_x$/YSZ according to XANES.

T [°C]	Oxidation state of Co in $Fe_{0.5}Co_{0.5}O_x$/YSZ		Oxidation state change
	Reduced	Re-oxidized	
450	0.00	1.49	1.49
600	0.00	0.71	0.71

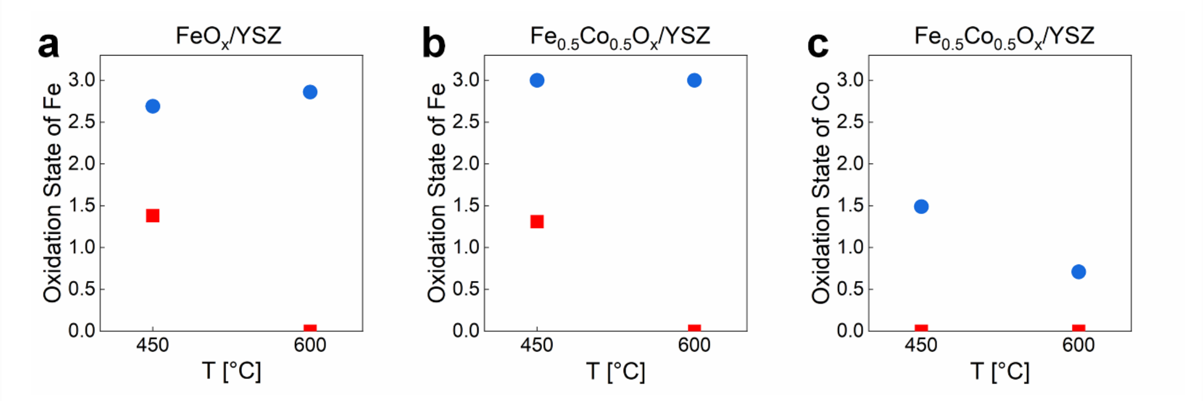

Figure S6: Oxidation states of a) Fe in FeO_x/YSZ, b) Fe in $Fe_{0.5}Co_{0.5}O_x$/YSZ, and c) Co in $Fe_{0.5}Co_{0.5}O_x$/YSZ in the NH_3-reduced (red squares) and steam-oxidized (blue circles) samples at 450°C and 600°C.

5. XRD Refinement

Refinement and Reference Intensity Ratio (RIR) methods in *PDXL* software were used to analyze the XRD data to quantify the phase compositions[5]. The Reference Intensity Ratio (RIR) method relies on the comparison of the observed intensities of phases in a sample to standard reference values, allowing for the quantification of phase fractions. Each phase in a sample has a reference intensity, obtained from standard databases such as the ICDD (International Centre for Diffraction Data)[6]. The RIR values help normalize the intensity data, allowing us to calculate the weight. The refinement results gave the mass ratio of identified phases; thus, by using stoichiometry and molar mass of different phases, the molar ratio of oxygen to redox active metal elements (Fe and Co) can be calculated for NH_3-reduced and steam-oxidized samples. The difference in this ratio between reduced and re-oxidized samples shows the sample's oxygen exchange capacity normalized by the active metal molar amount *(Eq. 3)*. The error bars of the refinement measurement are shown in *Table S5*.

Table S5: XRD refinement mass ratio of different phases and their error bars.

Phase	Weight ratio [-]	Relative error [%]	Phase	Weight ratio [-]	Relative error [%]
$Fe_{0.5}Co_{0.5}O_x$/YSZ reduced at 450°C			$Fe_{0.5}Co_{0.5}O_x$/YSZ re-oxidized at 450°C		
Fe-Co	0.440	11	Co	0.109	12
$(CoFe)_3O_4$	0.000	2	$(CoFe)_3O_4$	0.550	2
YSZ	0.560	8	YSZ	0.341	6
FeO_x/YSZ reduced at 450°C			FeO_x/YSZ re-oxidized at 450°C		
Fe	0.156	16	Fe	0.000	2
Fe_3O_4	0.550	4	Fe_3O_4	0.712	7
YSZ	0.294	3	YSZ	0.288	7
$Fe_{0.5}Co_{0.5}O_x$/YSZ reduced at 600°C			$Fe_{0.5}Co_{0.5}O_x$/YSZ re-oxidized at 600°C		
Fe-Co	0.479	12	Co	0.148	15
$(CoFe)_3O_4$	0.000	3	$(CoFe)_3O_4$	0.600	3
YSZ	0.521	12	YSZ	0.252	4
FeO_x/YSZ reduced at 600°C			FeO_x/YSZ re-oxidized at 450°C		
Fe	0.586	5	Fe	0.000	2
Fe_3O_4	0.000	3	Fe_3O_4	0.530	7
YSZ	0.414	6	YSZ	0.470	7

6. Method for Energy and Techno-economic Analyses: CLAOD-WS

For the looping scheme in *Figure 6a*, NH_3 is initially preheated in HX1 and then enters the reactor where it is oxidized and decomposed at 600°C. To more efficiently utilize the thermal energy of the NH_3 step's products, the plant is equipped with two heat exchangers to preheat the inlet NH_3 in HX1 and generate hot water in HX2. In the second reaction step, steam is used to re-oxidize

FeO_x/YSZ at 600°C, and then produced H_2 mixed with unreacted H_2O is directed to external applications (in this case, a H_2 fuel cell). A H_2 fuel cell only has product H_2O which can be directly fed back to the water-splitting reactor. Since water-splitting is an exothermic reaction, the dissipated thermal energy from this process, Q_2, is utilized in a hot water generator for further hot water production. Note that the only source of energy consumption in this scenario is the endothermic first step (Q_1). The duration of NH_3 and H_2O steps is the same and assumed to be 6 minutes each. It is also noted that since negligible amounts of NO_x gases were observed during our experiments, which can be avoided by starting with a reduced material, no NO_x treatment procedure was considered for the CLAOD-WS plant in this energy and techno-economic analyses.

In this section, the governing equations for the energy and economic analyses of the CLAOD-WS system are presented and solved using Python programming.

Table S6 shows the equipment items and their governing thermodynamic and sizing equations in the CLAOD-WS plant.

Table S6: CLAOD-WS plant equipment items and their equations[7, 8].

Equipment items	Thermodynamic equations	Sizing method
HX1	$\boldsymbol{\dot{Q}_{HX1} = \varepsilon_{HX1}\dot{Q}_{HX1,max}}$ $\boldsymbol{\dot{Q}_{HX1,max} = min(\dot{n}_1 c_{p,1,2}, \dot{n}_3 c_{p,3,4})(T_3 - T_1)}$ $\boldsymbol{LMTD_{HX1} = \frac{(T_3 - T_2) - (T_4 - T_1)}{Ln\left(\frac{T_3 - T_2}{T_4 - T_1}\right)}}$	$\boldsymbol{A_{HX1} = \frac{\dot{Q}_{HX1}}{U.LMTD_{HX1}}}$
HX2	$\boldsymbol{\dot{Q}_{HX2} = \varepsilon_{HX2}\dot{Q}_{HX2,max}}$	$\boldsymbol{A_{HX2} = \frac{\dot{Q}_{HX2}}{U.LMTD_{HX2}}}$

	$\dot{Q}_{HX2,max} = min(\dot{n}_4 c_{p,4,5}, \dot{n}_6 c_{p,6,7})(T_4 - T_6)$ $LMTD_{HX2} = \frac{(T_4 - T_7) - (T_5 - T_6)}{Ln\left(\frac{T_4 - T_7}{T_5 - T_6}\right)}$	
Reactor	$\dot{Q}_1 = \left(\dot{n}_3 c_{p,3} - \dot{n}_2 c_{p,2}\right) T_3$ $\dot{Q}_2 = \left(\dot{n}_9 c_{p,9} - \dot{n}_8 c_{p,8}\right) T_9$	$m_{solid} = \frac{\dot{m}_{H_2,step1} \cdot \Delta t_{step1} \cdot \frac{M_{FeO_x}}{M_{H_2}} \cdot \frac{n_{FeO_x}}{n_{H_2}}}{1 - wt\%_{YSZ}}$ M: molar mass [kg/mol] n: reaction stoichiometry
Hot Water Generator	$\dot{Q}_{HWG} = \varepsilon_{HWG} \dot{Q}_2$	$A_{HWG} = \frac{\dot{Q}_{HWG}}{U(T_{11} - T_{10})}$

Table S7 shows the input parameters for the CLAOD-WS plant model.

Table S7: Input parameters for the CLAOD-WS plant.

Parameter	Value	Description
T_0	30 [°C]	Ambient temperature
P_0	101,325 [Pa]	Ambient pressure
T_1	30 [°C]	Temperature at stream 1
T_2	571.5 [°C]	Temperature at stream 2
T_3	600 [°C]	Temperature at stream 3
T_4	211.5 [°C]	Temperature at stream 4
T_5	42 [°C]	Temperature at stream 5

$\boldsymbol{T_{6}}$	30 [°C]	Temperature at stream 6
$\boldsymbol{T_{7}}$	93.3 [°C]	Temperature at stream 7
$\boldsymbol{T_{8}}$	600 [°C]	Temperature at stream 8
$\boldsymbol{T_{9}}$	600 [°C]	Temperature at stream 9
$\boldsymbol{T_{10}}$	30 [°C]	Temperature at stream 10
$\boldsymbol{T_{11}}$	90 [°C]	Temperature at stream 11
$\boldsymbol{X_{1}}$	90 [%]	NH_3 conversion
$\boldsymbol{X_{2}}$	40 [%]	Steam conversion
$\boldsymbol{\varepsilon_{HX1}}$	95 [%]	HX1 effectiveness
$\boldsymbol{\varepsilon_{HX2}}$	95 [%]	HX2 effectiveness
$\boldsymbol{\varepsilon_{HWG}}$	95 [%]	Hot water generator effectiveness
$\boldsymbol{\eta_{eth}}$	90 [%]	Electrical-to-thermal energy conversion efficiency
$\boldsymbol{U}$	300 [$W/m^2.K$]	Overall heat transfer coefficient (gas-gas/steam)

Table S8 shows the results of the energy analysis on the CLAOD-WS plant. The mass of the solid was calculated based on the stoichiometry of the reaction and step durations in a way that the amount of oxygen exchange in the metal oxide satisfies the plant's H_2 production capacity (10 MTPD); additionally, the amount of support was calculated to be 30% of the total mass (Fe_3O_4+YSZ). The total mass of solid in the reactor was calculated to be 861.52 kg. Fe_3O_4 - Fe was chosen as the oxygen carrier and catalyst for the looping model as we observed from our experimental looping tests and XRD phase analysis (*Figures 4g* and *4h*) that FeO_x is reduced to Fe by NH_3 and re-oxidized to Fe_3O_4 by H_2O. Accordingly, the plant's total H_2 production rate per mass of active metal, Fe, is 0.1326 $\boldsymbol{mmol_{H_2}}/\boldsymbol{g_{Fe}.s}$.

Volume of solid in the reactor is calculated as below:

$$V\ [m^3] = \frac{m\ [kg]}{\rho\ [kg/m^3]} \qquad Eq.\ S5$$

In this equation the density of each material (ρ) is calculated based on the general method for theoretical composite density:

$$\frac{1}{\rho_{Fe_3O_4/YSZ}} = \frac{wt\%_{Fe_3O_4}}{\rho_{Fe_3O_4}} + \frac{wt\%_{YSZ}}{\rho_{YSZ}} \qquad Eq.\ S6$$

In this equation $\rho_{Fe_3O_4} = 5170$ and $\rho_{YSZ} = 6050\ kg/m^3$.

Table S8: Energy analysis results for the CLAOD-WS plant.

Parameter	Value	Description
$\boldsymbol{A_{HX1}}$	41.9 [m^2]	Area of HX1
$\boldsymbol{A_{HX2}}$	32.5 [m^2]	Area of HX2
$\boldsymbol{A_{HWG}}$	46.6 [m^2]	Area of HWG
$\boldsymbol{\dot{Q}_1}$	2.965 [MW]	Heat transfer in NH_3 step (endothermic)
$\boldsymbol{\dot{Q}_2}$	-0.884 [MW]	Heat transfer in steam step (exothermic)
$\boldsymbol{\dot{m}_{H_2,1}}$	0.058 [kg/s]	Mass flow rate of H_2 product in NH_3 step
$\boldsymbol{\dot{m}_{H_2,2}}$	0.058 [kg/s]	Mass flow rate of H_2 product in steam step
$\boldsymbol{\dot{m}_1}$	0.729 [kg/s]	Mass flow rate of inlet NH_3
$\boldsymbol{\dot{m}_8}$	1.302 [kg/s]	Mass flow rate of inlet H_2O
$\boldsymbol{\dot{m}_7}$	1.706 [kg/s]	Mass flow rate of produced H_2O (90°C and 101,325 Pa) in HX2

$\dot{m}_{11}$	3.341 [kg/s]	Mass flow rate of produced H_2O (90°C and 101,325 Pa) in HWG
m_{solid}	861.52 [kg]	Mass of Fe_3O_4/YSZ in reactor
ρ_{solid}	5400 [kg/m^3]	Density of Fe_3O_4/YSZ
V_{solid}	0.1594 [m^3]	Volume of Fe_3O_4/YSZ in reactor

After the thermodynamic analysis, cost analysis was conducted. The proposed plant has four types of cost, including equipment (installation, operation, and maintenance), material (NH_3, H_2O, Fe_3O_4/YSZ), labor, and energy (thermal energy in NH_3 step). *Table S9* shows the cost functions of equipment used to calculate annual costs.

Table S9: Cost functions of equipment for the CLAOD-WS plant[7-14]*.*

Component	Cost equations
HX1	$C_{HX1} = FOB_{HX,ref}\left(\frac{A_{HX1}}{A_{HX,ref}}\right)^{0.71}\frac{CEPCI}{1000}[0.2006exp(0.002567T_3)]F_{i,HX1}f_{i,HX1}F_{mnt}(1+F_o)\frac{CRF}{F_u}$
HX2	$C_{HX2} = FOB_{HX,ref}\left(\frac{A_{HX2}}{A_{HX,ref}}\right)^{0.71}\frac{CEPCI}{1000}[0.2006exp(0.002567T_4)]F_{i,HX2}f_{i,HX2}F_{mnt}(1+F_o)\frac{CRF}{F_u}$
Reactor	$C_R = FOB_{R,ref}\left(\frac{V_{solid}}{V_{ref}}\right)^{0.68}\frac{CEPCI}{1000}[0.7561exp(0.0006982T_3)]F_{i,R}f_{i,R}F_{mnt}(1+F_o)\frac{CRF}{F_u}$
Hot Water Generator	$C_{HWG} = FOB_{HWG,ref}\left(\frac{A_{HWG}}{A_{HWG,ref}}\right)^{0.71}\frac{CEPCI}{1000}[0.2006exp(0.002567T_{11})]F_{i,HWG}f_{i,HWG}F_{mnt}(1+F_o)\frac{CRF}{F_u}$

Table S10 shows the input parameters for the CLAOD-WS plant cost analysis.

Table S10: Input parameters for the CLAOD-WS plant cost analysis[7-14]*.*

Parameter	Value	Description
$\boldsymbol{CEPCI}$	725 [-]	Chemical Engineering Plant Cost Index for the year 2030
$\boldsymbol{FOB_{HX,ref}}$	70,000 [$]	Free on Board - the cost of HX at the shipping point
$\boldsymbol{A_{HX,ref}}$	100 [m^2]	Area of the reference HX
$\boldsymbol{F_{i,HX1}}$	3.5 [-]	HX1 installation factor
$\boldsymbol{f_{i,HX1}}$	0.7 [-]	HX1 material factor
$\boldsymbol{F_{i,HX2}}$	3.5 [-]	HX2 installation factor
$\boldsymbol{f_{i,HX2}}$	1.6 [-]	HX2 material factor
$\boldsymbol{FOB_{R,ref}}$	350,000 [$]	Free on Board - the cost of reactor at the shipping point
$\boldsymbol{V_{ref}}$	3 [m^3]	Volume of solid in a reference reactor setup
$\boldsymbol{F_{i,R}}$	4 [-]	Reactor installation factor
$\boldsymbol{f_{i,R}}$	0.85 [-]	Reactor material factor
$\boldsymbol{FOB_{HWG,ref}}$	70,000 [$]	Free on Board - the cost of hot water generator (HWG) at the shipping point
$\boldsymbol{A_{HWG,ref}}$	100 [m^2]	Area of the reference HWG
$\boldsymbol{F_{i,HWG}}$	3.5 [-]	HWG installation factor
$\boldsymbol{f_{i,HWG}}$	1.7 [-]	HWG material factor
$\boldsymbol{F_{mnt}}$	1.04 [-]	Maintenance factor
$\boldsymbol{F_o}$	0.4 [-]	Offsite capital cost factor
$\boldsymbol{F_u}$	0.95 [-]	Continuous operation factor
$\boldsymbol{i}$	10 [%]	Interest rate
$\boldsymbol{n}$	20 [yr]	Number of operation years

$\boldsymbol{CRF}$	0.1175 [-]	Capital recovery factor: $\boldsymbol{CRF = \frac{i(1+i)^n}{(1+i)^n - 1}}$

The next step in techno-economic analysis is to evaluate the cost of inlet materials in the plant. Our proposed CLAOD-WS plant requires NH_3 (inlet of NH_3 step), H_2O (hot water generation in HX2 and HWG), and FeO_x/YSZ which cost \$0.3, \$0.000893, and \$6.723/kg, respectively[13, 15]. The solid material is assumed to be replaced 4 times per year[11]. Additionally, the effect of oxygen carrier/catalyst replacement frequency was investigated. If this frequency was increased from once per year to once per two weeks (26 times per year), there would be minor increase in annual gas and materials cost (2.1% increase) and LCOH (1.7% increase).

The cost of labor is the salary paid to one operator over the year at the rate of \$38.5/hr.

Lastly, the cost of energy consumption was analyzed under the scenario in which the thermal energy is converted from utility scale renewable grids. As the current analysis focuses on the chemical system comparison between CLAOD-WS and direct NH_3 decomposition, we do not include the electricity generation equipment in our system but we consider the costs of electricity from utility scale renewable grid, including utility-scale PV-plus-battery, land-based wind, and concentration solar power[16-19]. Then we can obtain thermal energy cost by dividing electricity price by η_{eth} = 90%, and we get a range of \$0.017 to 0.090/kWh_{th}[16-19]. For this study, the cost of \$0.059/kWh_{th}[17] was considered according to utility-scale PV-plus-battery. This technology includes the cost of energy supply plus storage (PV plus battery, class 5, moderate case, market, PTC+ITC, 2030)[7].

Electricity-driven thermochemical reactors are gaining attention in industrial chemical plants, as they are able to provide high temperatures (up to and above 1000°C)[20]; such a reactor is used for the chemical looping system in this analysis.

According to the cost analysis, the total cost of a CLAOD-WS plant is \$8.64M/yr. Considering this plant's H_2 production capacity of 10 MTPD (metric tons per day), the levelized cost of H_2 is evaluated to be \$2.5/kg-H_2 (*Eq. S7*).

$$LCOH = \frac{C_{tot.}}{\dot{m}_{H_2,tot.}} \qquad \text{Eq. S7}$$

The investment cost of this plant based on its different components is shown in *Table S11*. In this table, the investment costs of different components in the chemical looping plant are shown. It needs to be clarified that these investment costs include the installation factor (F_i), which is commonly used to estimate the cost of items in addition to the cost of equipment, such as:

- Equipment foundation and minor structural work,
- Piping, insulation, and painting,
- Instruments and automatic process control (APC) systems,
- Process building and structures,
- Utilities and site preparation.

Using installation factors have been developed and explained in books by Sinnott[21], Towler and Sinnott[22], and Turton[23].

Table S11: Investment cost of the CLAOD-WS plant and its components.

Component	Investment cost [$]

HX1	177,070
HX2	124,781
Reactor	228,351
Hot Water Generator	125,337
Total	658,539

As an instance for equipment cost calculations, for the reactor, a H_2 production rate of 10 MTPD was assumed for each plant (CLAOD-WS and NH_3 decomposition). Based on a 90% conversion of NH_3 to H_2, and the relationship provided in *Table S6*, the required mass of solid material (m_{solid}) in the reactor was calculated. Using a density of 5400 kg/m^3 for the Fe_3O_4/YSZ (30wt%), the corresponding solid volume (V_{solid}) was estimated. Furthermore, a cost function for the reactor in Table S9 was employed, based on the guidelines from *Rules of Thumb in Engineering Practice* by Donald R. Woods[14], to provide an estimation of the reactor's investment and operating costs.

7. Method for Energy and Techno-economic Analyses: Catalytic NH_3 Decomposition

For the second scenario in *Figure 6b*, NH_3 is preheated in HX1 and HX2 before entering the decomposition reactor where H_2 and N_2 are produced and mixed with unreacted NH_3. Fe/YSZ is used as the catalyst in the reactor. Since in the looping scenario, half of the produced H_2 is at high purity and can be used in more sensitive applications such as fuel cells, half of the stream leaving the decomposition reactor will be directed to a H_2 separation unit to purify H_2. Additionally, the other half of the product stream passes through HX2 to preheat the inlet NH_3, and the N_2 and NH_3 separated from H_2 also preheat the inlet NH_3 in HX1.

For the separation unit, two cases were studied: 1) Electrochemical membrane (Pd-Ag/ceramic support)[9, 12, 24], and 2) Pressure Swing Absorption (PSA)[12, 24].

In this section, the governing equations for the energy and economic analyses of the catalytic NH_3 decomposition systems are presented and solved using Python programming.

Table S12 shows the components and their governing thermodynamic and sizing equations in the NH_3 decomposition plant equipped with a separation unit. For the reactor, the sizing was based on the mass of the solid which was calculated in a way that the molar amount of Fe was the same as the molar amount of Fe in the looping reactor; additionally, the amount of support was calculated to be 30% of the total mass. For the membrane, a reference area of 1.62 m^2 was considered as the baseline with a H_2 flux of 1.8×10^{-4} kg/(m^2.s) [9], and based on the ratio of the required H_2 production capacity to the reference capacity (25 kg/day), our membrane total area was scaled linearly according to *Eq. S8*.

$$r_M = \frac{A_M}{A_{M,ref}} = \frac{\dot{m}_{H_2,M}}{\dot{m}_{H_2,M,ref}} \qquad \textit{Eq. S8}$$

Table S12: Catalytic NH_3 decomposition plant components and their equations[7, 8, 11].

Component	Thermodynamic equations	Sizing equations
HX1	$\dot{Q}_{HX1} = \varepsilon_{HX1}\dot{Q}_{HX1,max}$ $\dot{Q}_{HX1,max} = min(\dot{n}_1 c_{p,1,2}, \dot{n}_7 c_{p,7,9})(T_7 - T_1)$ $LMTD_{HX1} = \frac{(T_7 - T_2) - (T_9 - T_1)}{Ln\left(\frac{T_7 - T_2}{T_9 - T_1}\right)}$	$A_{HX1} = \frac{\dot{Q}_{HX1}}{U.LMTD_{HX1}}$

HX2	$\dot{Q}_{HX2} = \varepsilon_{HX2} \dot{Q}_{HX2,max}$ $\dot{Q}_{HX2,max} = min(\dot{n}_2 c_{p,2,3}, \dot{n}_4 c_{p,4,8})(T_4 - T_2)$ $LMTD_{HX2} = \frac{(T_4 - T_3) - (T_8 - T_2)}{Ln\left(\frac{T_4 - T_3}{T_8 - T_2}\right)}$	$A_{HX2} = \frac{\dot{Q}_{HX2}}{U.LMTD_{HX2}}$
Reactor	$\dot{Q}_1 = \left(2\dot{n}_4 c_{p,4} - \dot{n}_3 c_{p,3}\right) T_3$	$m_{catalyst} = \frac{n_{Fe} M_{Fe}}{1 - wt\%_{YSZ}}$ M: molar mass [kg/mol] n: molar amount
H_2 separation membrane (case 1)	$\dot{W}_{HS} = \frac{\dot{n}_5 R T_{HS} \left(y_{H_2} Ln(y_{H_2}) + y_{N_2+NH_3} Ln(y_{N_2+NH_3})\right)}{\eta_{HS}}$	$A_M = 648\, m^2$
H_2 separation PSA (case 2)	$\dot{W}_C = \frac{\dot{m}_5 \frac{R}{k-1} T \left[r_p^{\frac{k-1}{k}} - 1 \right]}{\eta_C}$	PSA sizing is based on the power consumption of its compressor[25].

It is noted that two arrangements of heat exchangers (HX1 followed by HX2 or vice versa) were analyzed and negligible impact on the energy consumption and LCOH was observed; thus, only one arrangement (*Figure 6b*) was discussed.

Table S13 shows the input parameters for the NH_3 decomposition plant.

Table S13: Input parameters for the catalytic NH_3 decomposition plant.

Parameter	Value	Description
T_1	30 [°C]	Temperature at stream 1

$\boldsymbol{T_2}$	378.5 [°C]	Temperature at stream 2
$\boldsymbol{T_3}$	513.9 [°C]	Temperature at stream 3
$\boldsymbol{T_4}$	600 [°C]	Temperature at stream 4
$\boldsymbol{T_5}$	600 [°C]	Temperature at stream 5
$\boldsymbol{T_6}$	600 [°C]	Temperature at stream 6
$\boldsymbol{T_7}$	600 [°C]	Temperature at stream 7
$\boldsymbol{T_8}$	389.5 [°C]	Temperature at stream 8
$\boldsymbol{T_9}$	58.5 [°C]	Temperature at stream 9
$\boldsymbol{X}$	90 [%]	NH_3 conversion
$\boldsymbol{\varepsilon_{HX1}}$	95 [%]	HX1 effectiveness
$\boldsymbol{\varepsilon_{HX2}}$	95 [%]	HX2 effectiveness
$\boldsymbol{\eta_{HS}}$	20 – 100 [%]	H_2 separation membrane efficiency
$\boldsymbol{\eta_C}$	80 [%]	PSA compressor efficiency
$\boldsymbol{U}$	300 [W/m^2.K]	Overall heat transfer coefficient (gas-gas/steam)
$\boldsymbol{r_P}$	7 [-]	Pressure ratio in PSA compressor (from 100 to 700 kPa)

Table S14 shows the results of energy analysis on the NH_3 decomposition plant. Accordingly, the plant's H_2 production rate per mass of active metal, Fe, is identical to that of the looping plant and equal to 0.1326 $\boldsymbol{{}^{mmol_{H_2}}/_{g_{Fe}.s}}$.

Volume of solid in the reactor is calculated using *Eq. S5*. In this equation the density of each material (ρ) is calculated based on the general method for theoretical composite density:

$$\frac{1}{\rho_{Fe/YSZ}} = \frac{wt\%_{Fe}}{\rho_{Fe}} + \frac{wt\%_{YSZ}}{\rho_{YSZ}} \qquad \text{Eq. S9}$$

In this equation $\rho_{Fe} = 7870$ and $\rho_{YSZ} = 6050\ kg/m^3$.

Table S14: Energy analysis results for the catalytic NH_3 decomposition plant.

Parameter	Value	Description
$\boldsymbol{A_{HX1}}$	23.7 [m^2]	Area of HX1
$\boldsymbol{A_{HX2}}$	23.7 [m^2]	Area of HX2
$\boldsymbol{\dot{Q}_1}$	2.207 [MW]	Heat transfer in NH_3 decomposition
$\boldsymbol{\dot{W}_{HS}}$	0.237 – 0.047 [MW]	Power consumption in H_2 separation membrane ($\boldsymbol{\eta_{HS}}$ = 20 - 100%)
$\boldsymbol{\dot{W}_C}$	2.190 [MW]	PSA compressor power consumption
$\boldsymbol{\dot{m}_{H_2,1}}$	0.058 [kg/s]	Mass flow rate of H_2 product in step 1
$\boldsymbol{\dot{m}_{H_2,2}}$	0.058 [kg/s]	Mass flow rate of H_2 product in step 2
$\boldsymbol{\dot{m}_1}$	0.729 [kg/s]	Mass flow rate of inlet NH_3
$\boldsymbol{m_{catalyst}}$	623.39 [kg]	Mass of Fe/YSZ in reactor
$\boldsymbol{\rho_{catalyst}}$	7220 [kg/m^3]	Density of Fe/YSZ
$\boldsymbol{V_{catalyst}}$	0.0863 [m^3]	Volume of Fe/YSZ in reactor

Similar to the proposed CLAOD-WS plant, a cost analysis is conducted on the decomposition plant. *Table S15* shows the cost functions of equipment used to calculate annual costs.

Table S15: Cost functions of equipment for the catalytic NH_3 decomposition plant[7-14].

Component	Cost equations
HX1	$C_{HX1} = FOB_{HX,ref}\left(\frac{A_{HX1}}{A_{HX,ref}}\right)^{0.71}\frac{CEPCI}{1000}[0.2006exp(0.002567T_4)]F_{i,HX1}f_{i,HX1}F_{mnt}(1 + F_o)\frac{CRF}{F_u}$
HX2	$C_{HX2} = FOB_{HX,ref}\left(\frac{A_{HX2}}{A_{HX,ref}}\right)^{0.71}\frac{CEPCI}{1000}[0.2006exp(0.002567T_7)]F_{i,HX2}f_{i,HX2}F_{mnt}(1 + F_o)\frac{CRF}{F_u}$
Reactor	$C_R = FOB_{R,ref}\left(\frac{V_{catalyst}}{V_{ref}}\right)^{0.68}\frac{CEPCI}{1000}[0.7561exp(0.0006982T_3)]F_{i,R}f_{i,R}F_{mnt}(1 + F_o)\frac{CRF}{F_u}$
H_2 separation membrane (case 1)	$C_M = FOB_{M,ref}\left(\frac{A_M}{A_{M,ref}}\right)^{0.93}\frac{CEPCI}{1000}F_{m,M}F_{i,M}f_{i,M}F_{mnt}F_{RC,M}(1 + F_o)\frac{CRF}{F_u}$
H_2 separation PSA (case 2)	$C_{PSA} = \left(FOB_{PSA,ref}\left(\frac{\dot{m}_{N_2,5}}{\dot{m}_{N_2,ref}}\right)\frac{CEPCI}{1000}[0.7561exp(0.0006982T_5)]F_{i,PSA}f_{i,PSA} + FOB_{C,ref}\left(\frac{\dot{W}_C}{\dot{W}_{C,ref}}\right)^{0.9}\frac{CEPCI}{1000}F_{m,C}F_{i,C}f_{i,C}\right)F_{mnt}(1 + F_o)\frac{CRF}{F_u}$

Table S16 shows the input parameters for the decomposition plant cost analysis.

Table S16: Input parameters for the catalytic NH_3 decomposition plant cost analysis[7-13].

Parameter	Value	Description
$FOB_{M,ref}$	76,000 [\$]	Free on Board - the cost of membrane at the shipping point
$A_{M,ref}$	1.62 [m^2]	Reference surface area of membrane

$\dot{m}_{H_2,M,ref}$	25 [kg/day]	Reference H2 separation using membrane[9]
$F_{i,M}$	3.0 [-]	Membrane installation factor
$f_{i,M}$	0.52 [-]	Membrane material factor
$F_{RC,M}$	1.2 [-]	Membrane replacement factor (every 5 years)
$FOB_{PSA,ref}$	260,000 [$]	Free on Board - the cost of PSA at the shipping point
$\dot{m}_{N_2,ref}$	21.2 [MTPD]	Reference N_2 mass flow rate in PSA
$F_{i,PSA}$	3.0 [-]	PSA installation factor
$f_{i,PSA}$	0.85 [-]	PSA material factor
$FOB_{C,ref}$	1,350,000 [$]	Free on Board - the cost of PSA compressor at the shipping point
$\dot{W}_{C,ref}$	1 [MW]	Reference compressor power
$F_{i,C}$	2.5 [-]	Compressor installation factor
$f_{i,C}$	0.8 [-]	Compressor material factor
$FOB_{R,ref}$	350,000 [$]	Free on Board - the cost of reactor at the shipping point
V_{ref}	3 [m^3]	Volume of solid in a reference reactor setup
$F_{i,R}$	4 [-]	Reactor installation factor
$f_{i,R}$	0.85 [-]	Reactor material factor

The next step in techno-economic analysis is to evaluate the cost of materials feedstock. The decomposition plant requires NH_3 and Fe/YSZ which cost $0.3 and 6.765/kg, respectively. The catalyst is assumed to be replaced by a new batch 4 times per year[11]. Additionally, the effect of catalyst replacement frequency was investigated. If this frequency was increased from once per year to once per two weeks (26 times per year), there would be minor increase in annual gas and materials cost (0.6% for membrane, 1.1% for PSA) and LCOH (1.6% for both cases).

The cost of labor is the same as the CLAOD-WS plant.

Lastly, the cost of energy consumption was analyzed under the scenario in which the thermal energy is converted from utility scale renewable grids. As the current analysis focuses on the chemical system comparison between CLAOD-WS and direct NH_3 decomposition, we do not include the electricity generation equipment in our system but we consider the costs of electricity from utility scale renewable grid, including utility-scale PV-plus-battery, land-based wind, and concentration solar power[16-19]. Then we can obtain thermal energy cost by dividing electricity price by η_{eth} = 90%, and we get a range of \$0.017 to 0.090/kWh_{th}[16-19]. For this study, the cost of \$0.059/kWh_{th}[17] was considered according to utility-scale PV-plus-battery. This technology includes the cost of energy supply plus storage (PV plus battery, class 5, moderate case, market, PTC+ITC, 2030)[7].

According to the cost analysis, assuming a 20% Second Law efficiency for H_2 separation membrane unit, the total cost of the decomposition plant is \$17.91 M/yr. Considering this plant's H_2 production capacity of 10 MTPD, the LCOH is evaluated to be \$5.1/kg-H_2.

In the catalytic decomposition plant, thermal energy is required for the decomposition reactor via electrical heating, and electrical energy is required for the separation units (membrane or PSA).

Electricity-driven thermochemical reactors are gaining attention in industrial chemical plants, as they are able to provide high temperatures (up to and above 1000°C)[20]; such a reactor is used for the catalytic NH_3 decomposition system in this analysis.

It is worth noting that the change in separation membrane efficiency will directly influence the energy consumption of this unit and its effect on installation and maintenance was beyond the scope of this study.

Under the second case in which the H_2 separation unit is PSA, the total cost of the plant is \$10.14 M/yr and the LCOH is \$2.9/kg-H_2.

The investment cost of these plants based on their different components is shown in *Table S17*. In this table, the investment costs of different components in the catalytic NH_3 decomposition plants are shown. It needs to be clarified that these investment costs include the installation factor (F_i), which is commonly used to estimate the cost of items in addition to the cost of equipment, such as:

- Equipment foundation and minor structural work,
- Piping, insulation, and painting,
- Instruments and automatic process control (APC) systems,
- Process building and structures,
- Utilities and site preparation.

Using installation factors have been developed and explained in books by Sinnott[21], Towler and Sinnott[22], and Turton[23].

Table S17: Investment cost of the catalytic NH_3 decomposition plants and their components.

Component	Investment cost [\$]	
	Equipped with Pd-Ag/ceramic membrane	Equipped with PSA
HX1	118,049	118,049
HX2	118,049	118,049
Reactor	141,673	141,673
Membrane	62,961,150	-

PSA	-	8,335,673
Total	63,338,921	8,713,443

As an instance for equipment cost calculations, for the reactor, a H_2 production rate of 10 MTPD was assumed. Based on a 90% conversion of NH_3 to H_2, and the relationship provided in *Table S12*, the required mass of solid material ($m_{catalyst}$) in the reactor was calculated. Using a density of 7220 kg/m^3 for the Fe/YSZ (30wt%), the corresponding solid volume ($V_{catalyst}$) was estimated. Furthermore, a cost function for the reactor in Table S15 was employed, based on the guidelines from *Rules of Thumb in Engineering Practice* by Donald R. Woods[14], to provide an estimation of the reactor's investment and operating costs.

References

1. Y.-Q. Gu, Z. Jin, H. Zhang, R.-J. Xu, M.-J. Zheng, Y.-M. Guo, Q.-S. Song and C.-J. Jia, *Journal of Materials Chemistry A*, 2015, **3**, 17172-17180.
2. C. W. Bale, E. Bélisle, P. Chartrand, S. Decterov, G. Eriksson, K. Hack, I.-H. Jung, Y.-B. Kang, J. Melançon and A. Pelton, *Calphad*, 2009, **33**, 295-311.
3. C. W. Bale, P. Chartrand, S. Degterov, G. Eriksson, K. Hack, R. B. Mahfoud, J. Melançon, A. Pelton and S. Petersen, *Calphad*, 2002, **26**, 189-228.
4. B. Ravel and M. Newville, *Journal of synchrotron radiation*, 2005, **12**, 537-541.
5. A. Sasaki, A. Himeda, H. Konaka and N. Muroyama, *Rigaku J*, 2010, **26**, 10-14.
6. S. Gates-Rector and T. Blanton, *Powder Diffraction*, 2019, **34**, 352-360.
7. A. Arjomand Kermani and E. Houshfar, *International Journal of Hydrogen Energy*, 2024, **52**, 177-189.
8. A. R. Razmi, A. R. Hanifi and M. Shahbakhti, *Renewable Energy*, 2023, **215**, 118996.
9. M. Nordio, S. A. Wassie, M. Van Sint Annaland, D. A. Pacheco Tanaka, J. L. Viviente Sole and F. Gallucci, *International Journal of Hydrogen Energy*, 2021, **46**, 23417-23435.
10. D. Leeson, N. Mac Dowell, N. Shah, C. Petit and P. S. Fennell, *International Journal of Greenhouse Gas Control*, 2017, **61**, 71-84.
11. S. Zhai, Ph.D., Stanford University, 2020.
12. S. Yun, J. Im, J. Kim, H. Cho and J. Lee, *Chemical Engineering Journal*, 2024, **491**, 151875.
13. C. Makhloufi and N. Kezibri, *International Journal of Hydrogen Energy*, 2021, **46**, 34777-34787.
14. D. R. Woods, *Rules of Thumb in Engineering Practice*, John Wiley & Sons, 2007.
15. Trading Economics, tradingeconomics.com/commodity/).
16. Annual Technology Baseline, (https://atb.nrel.gov/electricity/2024/technologies).

17. Annual Technology Baseline - Utility Scale PV plus Battery, (https://atb.nrel.gov/electricity/2024/utility-scale_pv-plus-battery).
18. Renewable Power Generation Costs in 2022, (https://www.irena.org/Publications/2023/Aug/Renewable-Power-Generation-Costs-in-2022).
19. Average renewable electricity generation cost worldwide in 2023, by energy source - Statista, (https://www.statista.com/statistics/478049/global-utility-scale-electricity-generation-cost-by-resource/).
20. Y. T. Kim, J.-J. Lee and J. Lee, *Chemical Engineering Journal*, 2023, **470**, 144333.
21. R. K. Sinnott, *Chemical Engineering Design*, 2005.
22. G. Towler and R. Sinnott, *Chemical engineering design: principles, practice and economics of plant and process design*, Butterworth-Heinemann, 2021.
23. R. Turton, R. C. Bailie, W. B. Whiting and J. A. Shaeiwitz, *Analysis, synthesis and design of chemical processes*, Pearson Education, 2008.
24. Z. Du, C. Liu, J. Zhai, X. Guo, Y. Xiong, W. Su and G. He, *Journal*, 2021, **11**.
25. R. N. Brown, *Compressors: Selection and sizing*, Gulf Professional Publishing, 1997.